

Substrate temperature changes during molecular beam epitaxy growth of GaMnAs

V. Novák,^{a)} K. Olejník, M. Cukr, L. Smrčka, Z. Remeš, and J. Oswald
Institute of Physics AS CR, Cukrovarnická 10, 162 53 Praha 6, Czech Republic

(Received 12 April 2007; accepted 29 August 2007; published online 25 October 2007)

Our band gap spectroscopy measurements reveal a remarkably big increase of the substrate temperature during the low-temperature molecular beam epitaxy growth of GaMnAs layers. With the help of numerical simulations we explain the effect as a consequence of changing absorption/emission characteristics of the growing epilayer. We discuss possibilities for reducing the substrate temperature variations during the growth. © 2007 American Institute of Physics.
 [DOI: 10.1063/1.2800798]

I. INTRODUCTION

The growth temperature is an important parameter determining the molecular beam epitaxy (MBE) grown ferromagnetic GaMnAs layers. Its optimum value depends on the Mn doping level.^{1–3} With increasing Mn density, the growth temperature has to be reduced in order to prevent Mn precipitation. At the same time, however, a certain minimum temperature is required to maintain the two-dimensional (2D) growth. The temperature adjustment is critical especially at high Mn doping levels where the temperature range for 2D growth becomes narrow. Unfortunately, an accurate determination of the substrate temperature for this temperature region is difficult. The GaAs substrate is transparent for low-temperature pyrometry and only a weak thermal coupling exists between a rotating substrate and a thermocouple.

The diffuse reflectance spectroscopy,⁴ also called band edge spectroscopy (BES), allows one to overcome the earlier problems and determine the substrate temperature with an appreciable accuracy. Previous applications of the BES have demonstrated, e.g., large temperature variations during the growth of smaller band gap layers on larger band gap substrates⁵ or due to heat flux transients associated with opening/closing the effusion cell shutters.⁶ The BES measurements discussed in this article reveal remarkable changes in the substrate temperature during the MBE growth of highly Mn-doped GaAs epilayers. Apart from the effect of effusion cell shutters, we argue that changes in the optical characteristics of the deposited epilayer play an important role in these temperature variations, especially when the samples are mounted on In-free sample holders.

II. EXPERIMENT

The experiments were performed in a Veeco Gen II MBE system. A 2-in. in diameter, semi-insulating 500 μm thick GaAs substrate was mounted on a molybdenum In-free sample holder by mechanically fixing the sample at the edges. No diffuser plate was inserted in between the substrate and the heater. The distance between the heater (2-in. PBN plate with tungsten filament inside) and the substrate

was about 10 mm. The band edge spectrometer (kSA BandiT) was mounted on the central pyrometer port, normal to the substrate. In this arrangement, the thermal radiation of the heater had sufficient intensity near the band gap wavelength to serve as a radiation source for the transmission measurement even at temperatures as low as 200 °C.

The low-temperature MBE-grown part of the studied epilayer consists of a 5 nm thick GaAs buffer and a 150 nm thick $\text{Ga}_{1-x}\text{Mn}_x\text{As}$ layer, with x varying from 2% to 7%. The Ga source temperature was 930 °C, corresponding to the growth rate of 0.27 ML/s. The Mn source temperature was varied between 770 and 830 °C. During the growth the substrate heater was supplied with a constant power, without any feedback temperature control. A reproducible initial substrate temperature of 182 ± 2 °C was obtained for the supplied heater power when using the same sample holder.

The BES temperature (T_{BES}) dependence on growth time is plotted in Fig. 1 for several Mn dopings. All curves have the following common features: (i) a small (<5 °C) increase of T_{BES} after opening the Ga source; (ii) a pronounced (40–60 °C) increase of T_{BES} after opening the Mn source; and (iii) a decrease of T_{BES} after closing the sources, eventually saturating at value well above the initial substrate temperature. Note that for all the measurements, substrate tempera-

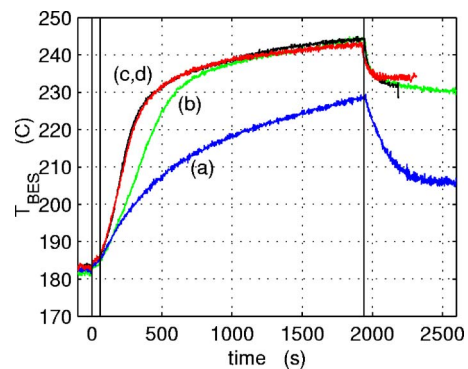


FIG. 1. (Color online) Temporal evolution of substrate temperatures measured by the band edge spectroscopy. The grown layers differ by the Mn contents of 2% (curve a), 3.5% (curve b), and 5% and 7% (curves c and d), respectively. Times $t=0$ (opening the Ga source), $t=60$ s (opening the Mn source), and $t=1950$ s (closing Ga and Mn sources) are indicated by vertical lines.

^{a)}Electronic mail: vit.novak@fzu.cz

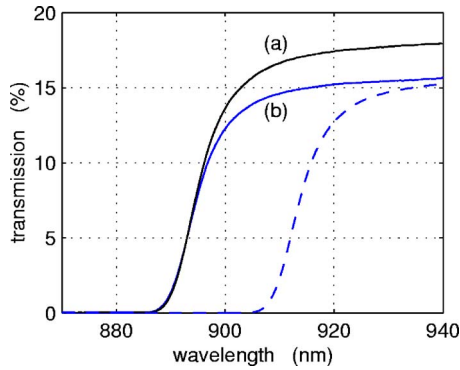


FIG. 2. (Color online) Near band gap transmission spectra of an undoped GaAs substrate (curve a) and the same substrate with a 50 nm thick GaMnAs layer with 7% Mn (curve b). Both curves were measured at room temperature. For contrast, curve (b) is repeated in the dashed line with a wavelength shift of $\Delta\lambda=19 \mu\text{m}$ which would correspond to increase of temperature from 200 to 250 °C (Ref. 5).

ture detected by the usual floating thermocouple behind the substrate showed only a weak increase by less than 3 °C during the growth and a comparable decrease after the growth was stopped.

To confirm the reliability of the BES temperature measurement technique in the presence of the GaMnAs film we show in Fig. 2 room-temperature, near-band edge transmission spectra of a reference semi-insulating GaAs substrate and of the same substrate with the GaMnAs epilayer grown on top of it. The differences between these two spectra are negligible when compared to the band edge shift caused by a temperature variation of 50 °C.^{4,7} T_{BES} can therefore be directly associated with the sample temperature during the growth.

We now analyze the dramatic difference between the temperature responses to opening the Ga and Mn sources which we attribute to an increasing heat absorption in the Mn-doped epitaxial layer. For the studied highly doped GaMnAs films with metallic conductivities, free carrier absorption should dominate and the relatively low mobilities imply significant spectral weight in a broad infrared frequency range.^{8,9} This is illustrated in Fig. 3 where transmission spectra between 1 and 25 μm are shown for various samples. Beside the free hole absorption the incoming heat is

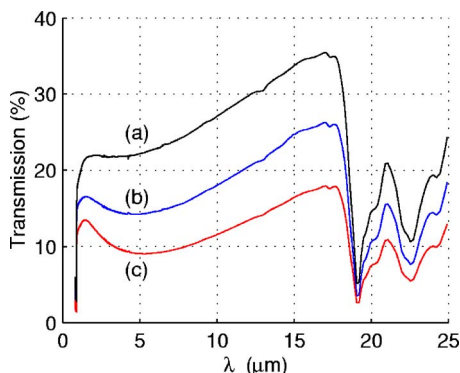


FIG. 3. (Color online) Infrared transmission spectra of undoped GaAs substrate and GaMnAs layers grown on the same substrate. Parameters of the samples are as follows: (a) undoped substrate; (b) 50 nm, 7% Mn; and (c) 150 nm, 7% Mn. All curves were measured at room temperature.

also absorbed by crystal lattice vibrations, a mechanism nearly independent of doping. A strong two-phonon absorption is seen in the long-wavelength part of Fig. 3. This absorption and its one-phonon analog¹⁰ around 35 μm are responsible for most of the heating of the insulating GaAs substrate.¹¹

III. MODEL SIMULATIONS

Naively, the heat exchange in the substrate is given by the difference between the heating term, proportional to heat flux from thermal sources, and with an absorption factor increasing with time, and the cooling term, proportional to the deviation from the steady state temperature. However, such a model turns out to be inadequate yielding results which are inconsistent with experiment. For example, it predicts an unbounded increase of the substrate temperature, as long as the absorption increases, i.e., until the layer becomes completely opaque. Figures 1 and 3 show different experimental characteristics, namely that the temperature stabilizes in spite of the unsaturated absorption. The behavior can be understood from Kirchhoff's law which states that the absorption efficiency of a body follows exactly its emission efficiency at each wavelength,¹² i.e., no temperature change can occur unless the radiation spectrum changes. Disregarding the spectral distribution in a system with significant radiative coupling, as in the earlier naive model, inevitably leads to nonphysical predictions.

An alternative model we propose assumes fully radiative heat exchange. Its essential ingredients are the proper description of the spectral power distributions of the thermal sources involved and the doping induced changes in the absorption and emission characteristics of the sample.

A radiating and absorbing material can be approximated by a blackbody model with spectral radiance (monochromatic emissive power) $R(\lambda)$ enclosed by a surface with dimensionless emittance $\epsilon(\lambda)$ and absorptance $\alpha(\lambda)$. The radiance $R(\lambda)$ obeys Planck law,

$$R(\lambda; T) = \frac{2\pi hc^2}{\lambda^5} \left[\exp\left(\frac{hc}{\lambda k_B T}\right) - 1 \right]^{-1}. \quad (1)$$

The net heat transferred from a radiating body "1" to an absorbing/radiating body "2" can then be described as

$$Q_{\text{net}} = F_{1-2} S_2 \int_0^{\infty} [\alpha_2(\lambda) \epsilon_1(\lambda) R_1(\lambda) - \epsilon_2(\lambda) R_2(\lambda)] d\lambda, \quad (2)$$

where the dimensionless factor F_{1-2} represents the geometric configuration of the two bodies and S_2 is the surface area of body 2. This general principle can be used to describe the heat exchange between the substrate and all other relevant thermal sources in the growth chamber.

To simplify the description we adopt the following assumptions: (i) The emittance of each body equals its absorptance, $\epsilon(\lambda) = \alpha(\lambda)$ (diffusive form of Kirchhoff's law¹²); (ii) the heater and the cells behave like gray bodies, i.e., their emittances are wavelength-independent constants; and (iii) the absorptance/emittance $\alpha_s(\lambda)$ of the substrate is composed of the phonon and the free carrier contributions. For simplicity, the phonons are assumed to absorb perfectly within the

corresponding wavelengths, $(\lambda_{p1}, \lambda_{p2})$. The free carrier contribution α_f is assumed to increase with time starting from zero in the undoped substrate and exponentially saturating as the total number of free holes increases

$$\alpha_s(\lambda) = \begin{cases} 1, & \lambda_{p1} < \lambda < \lambda_{p2} \\ \alpha_f = 1 - \exp(-k_f t), & \lambda \text{ elsewhere} \end{cases}, \quad (3)$$

where the rate constant k_f is proportional to dopant flux.

The parts of the growth chamber relevant for the heat exchange include the substrate heater (temperature T_h), the effusion cells opened during the growth (effective temperature T_c), the background of the growth chamber (effective temperature T_b), and the substrate (temperature T_s). The configuration factor F for each pair of parts can be approximated by the solid angles A_h, A_c, A_b , at which the substrate with area S_s “sees” the respective parts. Since the heater covers one complete hemisphere of the substrate’s scope and the other hemisphere corresponds to the background with small hot spots of the opened cells, we can assume that $A_h = A_b + A_c$. The heat balance in the substrate is then written as

$$Q_{\text{net}} = S_s \sum_i \int_0^\infty A_i [R(\lambda; T_i) - R(\lambda; T_s)] \alpha_s d\lambda, \quad (4)$$

$i = h, b, c.$

The absorptance $\alpha_s(\lambda)$ is a step function, with its phonon part lying in a narrow interval in the midinfrared range. Here Planck’s law can be approximated as $R \propto T/\lambda^4$ (Rayleigh–Jeans law), leading to terms linear in T when integrating Eq. (4). Planck’s law applied to the complete spectrum yields terms proportional to T^4 . Hence, after integrating Eq. (4) we obtain

$$Q_{\text{net}} = \sigma S_s \{ \alpha_f [T_h^4 + a_c T_c^4 + (1 - a_c) T_b^4 - 2T_s^4] + (1 - \alpha_f) \beta [T_h + a_c T_c + (1 - a_c) T_b - 2T_s] \}, \quad (5)$$

where σ is the Stefan–Boltzmann constant, $a_c = A_c/A_h$, and $A_b/A_h = 1 - a_c$. The constant factor β reflects the ratio of the power irradiated in the phonon domain and the power integrated over all wavelengths

$$\beta = \frac{5c^3 h^3}{\pi^4 k_B^3} (1/\lambda_{p2}^3 - 1/\lambda_{p1}^3). \quad (6)$$

Taking $\lambda_{p1} = 16.5 \mu\text{m}$ and $\lambda_{p2} = 18.5 \mu\text{m}$ provides an order of magnitude estimate of $\beta \sim 1 \times 10^7 \text{ K}^3$.¹³

In equilibrium, $Q_{\text{net}} = 0$ and Eq. (5) determines the steady state substrate temperature T_s for any given T_h, T_b, T_c , and α_f . Out of equilibrium, the time evolution of T_s is governed by

$$CdT_s/dt = Q_{\text{net}}, \quad (7)$$

where C is the constant heat capacity of the GaAs substrate. (Variations of the electronic specific heat can be safely neglected for the relevant temperatures.¹⁴)

If the change in temperature is slow enough the system remains quasistationary and $T_s(t)$ is obtained from $Q_{\text{net}} = 0$ with $\alpha_f(t)$ increasing with time according to Eq. (3). Explicit

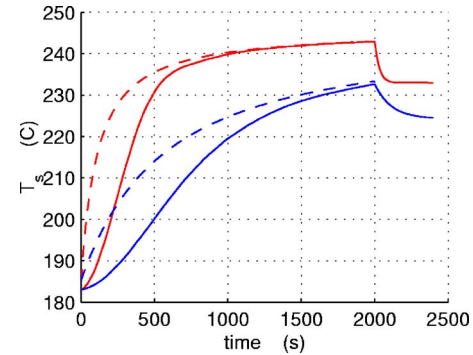


FIG. 4. (Color online) Calculated temperature evolutions of substrate temperatures of a strongly and a weakly doped layer (solid lines). The model parameters roughly correspond to growths with $x_{\text{Mn}} = 7\%$ and 2% from Fig. 1. Also shown are the corresponding quasistationary solutions (dashed lines).

solutions can be obtained in two special stationary cases: (i) For a negligible free electron absorption ($\alpha_f = 0$) Eq. (5) simplifies to

$$T_s = [T_h + a_c T_c + (1 - a_c) T_b] / 2. \quad (8)$$

When $a_c = 0$, i.e., in the steady state before the growth, $T_s = (T_h + T_b) / 2$. (ii) For prevailing free electron absorption [$\alpha_f T_s^4 \gg (1 - \alpha_f) \beta T_s$] we obtain

$$T_s^4 = [T_h^4 + a_c T_c^4 + (1 - a_c) T_b^4] / 2. \quad (9)$$

This implies that $T_s^4 = (T_h^4 + T_b^4) / 2$ in the steady state after growth, explaining the persistent increase of T_s as a consequence of the change of the absorption characteristics in the presence of two different thermal sources.

The earlier stationary solutions can be used to determine the model parameters from the measured data. In accordance with Fig. 1 we can take $T_s = 183 \text{ }^\circ\text{C}$ before the growth, $T_s = 243 \text{ }^\circ\text{C}$ at the end of the growth of the most highly doped layer, and $T_s = 233 \text{ }^\circ\text{C}$ long after closing the cells. Taking $a_c = 0.005$ for the opened cells, we can solve Eqs. (8) and (9) obtaining $T_h = 322 \text{ }^\circ\text{C}$ for the substrate heater temperature, $T_c = 954 \text{ }^\circ\text{C}$ for the effective temperature of the opened cells, and $T_b = 44 \text{ }^\circ\text{C}$ for the effective background temperature. An order of magnitude estimate of the rate constant k_f can be obtained when considering the fact that in the growth time the infrared (IR) transmission of the $x_{\text{Mn}} = 7\%$ layer becomes approximately one half of the transmission of the undoped substrate (see Fig. 3), yielding $k_f \approx 10^{-4} \text{ s}^{-1}$. Using $k_f = 1 \times 10^{-4} \text{ s}^{-1}$ and $0.2 \times 10^{-4} \text{ s}^{-1}$ (which roughly correspond to highly and weakly doped samples from Fig. 1) Eq. (5) yields quasistationary solutions for T_s shown in Fig. 4 by dashed lines. Taking, finally, $\sigma S_s C^{-1} = 1 \times 10^{-10} \text{ K}^{-3} \text{ s}^{-1}$ (which corresponds to the 2-in. GaAs substrate of a $500 \mu\text{m}$ thickness), Eqs. (5) and (7) provide the time-dependent T_s represented in Fig. 4 by the solid lines.

IV. DISCUSSION

Although qualitatively successful in reproducing the experimental data, our model cannot be expected to provide quantitatively accurate predictions for a wide range of input parameters, as it completely ignores numerous factors. For

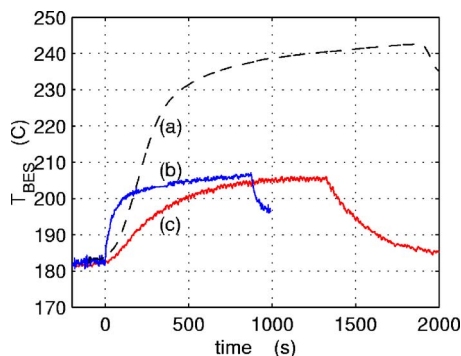


FIG. 5. (Color online) Substrate temperature evolution during growth of $x_{\text{Mn}}=7\%$ layers on (a) the In-free mounted substrate, (b) the In-free mounted sandwich structure with a buried GaMnAs heating layer, and (c) the In-bonded substrate. The buried heating layer in (b) is 150 nm thick with $x_{\text{Mn}}=5\%$, separated by 25 nm GaAs from the top GaMnAs layer.

example, a part of the heat exchange takes place through a conduction between the sample holder and other massive parts of the holder mechanism, all of which have their specific heat capacities; the free electron absorption is wavelength dependent in the IR range; all surfaces exposed to material fluxes change their absorptance/emissivity during the growth, leading to changes of their temperatures; neither the phonon domain is completely absorbing, nor the near infrared absorption is completely absent in the undoped substrate; reflection takes place, etc.

Despite these limitations our work shows several ways which can be used to eliminate or reduce the increase of the substrate temperature during the low-temperature MBE growth:

- (1) BES-locked substrate heater control;
- (2) anticipatory throttling of the substrate heater;
- (3) In bonding of the substrate to a massive sample holder with inherently strong IR absorption; and
- (4) incorporation of a less doped (uncritical in temperature) but sufficiently absorbing GaMnAs sublayer between the GaAs substrate and the final GaMnAs structure.

Temperature evolutions of the In-bonded substrate and the structure with the buried GaMnAs heating layer are shown in Fig. 5. The curves differ in their time constants, pointing to different heat capacities, however, for each of these two systems the increase in sample temperature during growth was slashed to one half of the increase seen by the layers grown on the In-free mounted semi-insulating substrates (see Fig. 1). This illustrates the difference between systems with a significant infrared absorptance (such as the In-bonded substrates or sandwiched structures with a buried heating layer) and systems where a wide-range infrared absorptance is initially missing (such as the In-free mounted semi-insulating substrates). In the first case the temperature increase is solely due to activation of an additional thermal source; the wide-range infrared absorption is already prevailing and its further change (if any) does not affect the heat-exchange balance. Within the presented model, terms linear in T are negligible compared to terms proportional to T^4 .

In the second case the change of the spectrum of the substrate absorptance/emittance is essential. The change in

the temperature corresponds to a shift of the absorption maximum from longer to shorter wavelengths. Within the presented model, the heat exchange is initially dominated by terms linear in T , while at later times the T^4 -terms prevail. The corresponding temperature increase would occur even if no additional heat flux was present. On the other hand, in a system with negligible absorption at shorter wavelengths, opening a high temperature cell with small orifice has little or no effect on the absorbed heat. Thus, an interesting paradox can occur: temperature variations in an In-bonded substrate can be larger than those in an In-free mounted substrate with a weak free-carrier absorption.

V. SUMMARY

The main part of the dramatic increase in the substrate temperature could unambiguously be connected with the heavy Mn doping via the following mechanism: (i) Before the growth, the undoped substrate absorbs the radiation from the thermal sources mainly in the midinfrared range (phonon domain). (ii) The doping leads to strongly enhanced free-carrier absorption in the near-infrared range, shifting the decisive spectral absorptance toward the shorter wavelengths. (iii) More heat is absorbed from the high-temperature (short wavelength) sources. To reach a new heat-exchange equilibrium, the substrate radiance has to shift accordingly, therefore its temperature increases.

The proposed model, in contrast to a linear cooling model, explains all the main features of the observed effect. Moreover, all the model parameters have a clear physical meaning and a choice of physically plausible input values leads to qualitatively correct results. The model also provides generic suggestions for improving temperature stability during the MBE growth. Especially, it sheds a new light on behavior of In-bonded and In-free mounted substrates and it proves the radiative heating of the In-free bonded substrates to dominate even at low growth temperatures.

ACKNOWLEDGMENTS

We gratefully acknowledge stimulating discussions with R. P. Campion, as well as his contribution to the early stages of this work. The work was done in the framework of AV0Z1-010-914 program, supported by Grant Nos. GACR 202/04/1519, ASCR KAN400100625, MoE LC510, and FON/06/E001 (ESF Eurocores-FoNE ERAS-CT-2003-980409).

¹H. Ohno, *Science* **281**, 951 (1998).

²J. Sadowski, J. Z. Domagala, J. Bak-Misiuk, S. Kolesnik, M. Sawicki, K. Swiatek, J. Kanski, L. Ilver, and V. Ström, *J. Vac. Sci. Technol.* **18**, 1697 (2000).

³R. P. Campion, K. W. Edmonds, L. X. Zhao, K. Y. Wang, C. T. Foxon, B. L. Gallagher, and C. R. Staddon, *J. Cryst. Growth* **251**, 311 (2003).

⁴S. R. Johnson, C. Lavoie, T. Tiedje, and J. A. Mackenzie, *J. Vac. Sci. Technol. B* **11**, 1007 (1993).

⁵B. V. Shanabrook, J. R. Waterman, J. L. Davis, and R. J. Wagner, *Appl. Phys. Lett.* **61**, 2338 (1992).

⁶P. Thompson, Y. Li, J. J. Zhou, D. L. Sato, L. Flanders, and H. P. Lee, *Appl. Phys. Lett.* **70**, 1605 (1997).

⁷S. R. Johnson and T. Tiedje, *J. Appl. Phys.* **78**, 5609 (1995).

⁸T. Jungwirth, J. Sinova, A. H. MacDonald, B. L. Gallagher, V. Novák, K.

W. Edmonds, A. W. Rushforth, R. P. Campion, C. T. Foxon, L. Eaves, K. Olejník, J. Mašek, S.-R. Eric Yang, J. Wunderlich, C. Gould, L. W. Molenkamp, T. Dietl, and H. Ohno, *Phys. Rev. B* **76**, 125206 (2007).

⁹P. Y. Yu and M. Cardona, *Fundamentals of Semiconductors*, 1st ed. (Springer, Berlin, 1996), pp. 296–297.

¹⁰J. S. Blakemore, *J. Appl. Phys.* **53**, R123 (1982).

¹¹The interband absorption is negligible: a substrate heater at 300 °C radiates by factor 10^{-6} less power in the band gap region than in the one

and two phonon regions.

¹²J. H. Lienhard IV and J. H. Lienhard V, *A Heat Transfer Textbook* (Phlogiston, Cambridge, 2006), p. 534.

¹³Used wavelengths correspond to two-phonon domain according to Ref. [10](#); one phonon domain has been neglected. Using the somewhat longer wavelengths according to Fig. [3](#) one would obtain $\beta=6 \times 10^6 \text{ K}^3$.

¹⁴N. W. Ashcroft and N. D. Mermin, *Solid State Physics* (Thomson Brooks/Cole, 1976), pp. 463–464.